Chemical Engineering Journal 146 (2009) 79–85

Contents lists available at ScienceDirect

Chemical Engineering Journal

journal homepage: www.elsevier.com/locate/cej

Photocatalytic degradation of furfural by titania nanoparticles in a floating-bed photoreactor

Mohammad Faramarzpour[a], Manouchehr Vossoughi[a,b,*], Mehdi Borghei[a]

[a] Department of Chemical and Petroleum Engineering, Sharif University of Technology, Tehran, Iran
[b] Institute for Nano-science and Nano-technology, Sharif University of Technology, Tehran, Iran

ARTICLE INFO

Article history:
Received 22 August 2007
Received in revised form 14 May 2008
Accepted 15 May 2008

Keywords:
Photocatalytic degradation
Furfural
Titanium dioxide (TiO_2)
Perlite

ABSTRACT

In this research, an attempt was made to investigate the potential of nanophotocatalysts for treatment of hazardous wastewater streams. Titanium dioxide nanoparticles (as photocatalyst) were immobilized on a porous and low-density support called "perlite" using a very simple and inexpensive method. TiO_2-coated perlite granules were used in a "Floating-bed photoreactor" to study the photocatalytic purification process of a typical wastewater polluted by furfural.

The effects of initial concentration, catalyst mass/solution volume ratio, oxidant molar flow, residence time, and light intensity on process removal efficiency, and kinetics of the reactions were studied.

SEM analyses showed a properly uniform distribution of titanium dioxide nanoparticles on perlite granules. HPLC analyses of the photocatalytic treatment experiments of water streams synthetically polluted with furfural showed a fairly good performance for the immobilized catalyst.

A furfural concentration reduction of more than 95% was observed within 120 min. Kinetics of the reaction, strongly depends on pollutant concentration in the solution and mass diffusion phenomenon seems to be the controlling step.

1. Introduction

Photocatalytic oxidation has been studied since 1970 as a method to remove hazardous substances. It has also been proposed since 1980 as an effective method for treatment of toxic and polluted water [1]. A lot of studies have been conducted to investigate the capacities of this phenomenon in air, water and soil detoxification and decontamination. These studies dealt with a vast range of organic pollutants such as aromatics (especially phenol and its derivatives), furfural, alkanes, cycloalkanes, alkenes, dyes, pesticides, herbicides, cyanides, etc. [1–23]. In some studies also the effects of hydrochloric acid catalyst pretreatments on degradation of benzene, toluene and xylene in gas phase were investigated [9,10]. In some studies degradation of more easily photodegradable organic pollutants like acetylene in presence of either titanium dioxide powders in a slurry type photoreactor or immobilized titanium dioxide were investigated [11]. In some other studies photodegradation of different types of dyes by means of titanium dioxide suspensions were investigated in liquid phase [12,13]. In some studies, photocatalysis was investigated in presence of sun light instead of UV light, by means of different kinds of titanium dioxide [14–16]. Studying the potentials of photocatalysis for water disinfection was also investigated in some researches during the last decade [17].

Among all newly developed detoxification methods, heterogeneous photocatalytic oxidation is becoming more and more popular each day [18]. In order to run such a process, the photocatalyst has to be immobilized on a proper support. One of the photocatalysts which has received a great deal of attention from research circles, is titanium dioxide (TiO_2) [19]. Among the metal oxide semiconductors suitable for photocatalytic processes, TiO_2 in its anatase form is the most broadly used one because, it is highly active, available, and chemically resistant in all reaction conditions [20]. There are different supports on which titanium dioxide has been immobilized. In some studies, titanium dioxide is immobilized on activated carbon as an efficient system in organic photodegradation practices [21,22]. In some other papers titania immobilization was conducted on glass, quarts and stainless steel supports [23].

There are different TiO_2 immobilization techniques for example: spray coating, CVD, sol–gel methods, sputtering, dip coating from suspension, and electrophoretic deposition [8].

So far, a lot of studies and experiments have been conducted to investigate the potentials of photocatalytic oxidation of pollutants existing in aqueous phase. Different pollutants, different photoreactors, and different catalyst supports have been tried. Pollutants

* Corresponding author at: Department of Chemical and Petroleum Engineering, Sharif University of Technology, Tehran, Iran. Fax: +98 2166165487.
E-mail address: vosoughi@sharif.edu (M. Vossoughi).

1385-8947/$ – see front matter.
doi:10.1016/j.cej.2008.05.033

such as: aromatics, cyanide compounds, and dyes, and photoreactors like: thin film, fluidized-bed, and slurry type, and finally some supports including: ceramics, granular activated carbon, glass slabs, and fiber glass were mostly used by researches.

Slurry type photoreactors use the catalyst particles suspended in the liquid phase, making the separation and catalyst recovery process too difficult. Thin film photoreactors in which a thin film of catalyst is usually attached to a fixed glass, quarts or metal slab or tube have lower removal efficiencies but, heterogeneous photocatalysis which includes using supported catalysts shows very good potentials for wastewater purification [18–20]. Supports have to be inert, corrosion and erosion resistant, and they have to have a good surface area with an ability to keep the coated catalyst, so that the catalyst particles do not leave the support and act as suspended catalysts. Perlite is the selected support in this study because we believe that it fulfills all the required features for a proper support.

Perlite is an inert, porous, low density, abundant and cheap substance. It is a volcanic glass able to expand 4–20 times its original volume, upon heating resulting in flakes with a porosity greater than 95% [24]. After expansion its density would be less than unity so that it can be easily floated on the water.

A floating-bed photoreactor includes a floating-bed of low-density supports, coated with a photocatalyst. Light is irradiated from the top, without facing any barrier but the air and dust and the reactants transfer from the balk to the support surface. Aeration and recirculation mechanisms (if included) would promote a better mass diffusion and cause the supports change their position and face the light. Perlite is a good choice for such a reactor for its low density and small granule size which eases its movements that are important in order to face the light source.

Furfural is an organic substance which is used as essence, fuel additive, pharmaceutical raw material, solvent, and impregnating agent. This substance is harmful in contact with skin and is toxic when it is inhaled or swallowed; it also shows some limited carcinogenic effects. It can be easily absorbed through the skin and must not be released in sewer and water bodies. In the case of long-term exposure it leads to liver enlargement, feeling of weakness, skin rash or inflammation, tremor and nose bleeding [25].

In the last step of furfural production it usually evaporates with water and is separated from water by condensation. This condensed water may contain a very low concentration of furfural which is better to be removed, before the water is discharged to the nature.

2. Materials and methods

2.1. Immobilization of titanium dioxide on perlite granules

In order to immobilize titania nanoparticles on perlite granules, the technique described in previous paper of this research group [8] was adopted. Perlite granules were weighed before and after catalyst immobilization in order to determine the amount of catalyst immobilized on perlite granules.

2.2. Materials

The UV sources utilized in photoreactors included a 30 W (Ø30 mm × 550 mm, medium pressure, 254 nm, Osram, Germany) and a 125 W (Ø13 mm × 50 mm, medium pressure, 254 nm, Osram, Germany) UV lamp.

Furfural (99.9%) was purchased from Merck, Germany. The deionized water (EC = 0.055 μs) to make furfural solutions of different concentrations was obtained from an SG, Germany deionizer. The oxidizing agents included hydrogen peroxide (30%) and sodium oxalate (99%); both purchased from Merck, Germany.

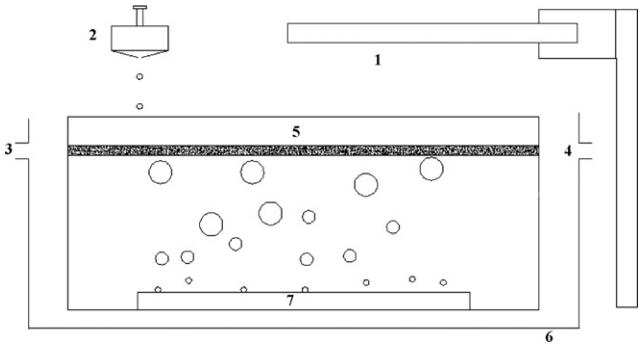

Fig. 1. Scheme of the utilized floating-bed photoreactor. (1) Adjustable UV lamp; (2) chemical feed; (3) cooling water inlet; (4) cooling water outlet; (5) floating bed; (6) reactor jacket.

The samples were analyzed by means of a Waters 1880 (Germany) HPLC analyzing apparatus with a solvent phase consisted of water–acetonitryl (Merck, Germany, 99.9%) solution.

2.3. Photoreactor

The photoreactor used in this work included a 280 mm × 115 mm × 70 mm jacketed glass box without the upper face; a 125 or 30 W UV lamp which was adjusted 100 mm above the floating bed in all cases; an air diffuser at the bottom of the glass box; a chemical injector and a sampling port. Fig. 1 shows a scheme of utilized photoreactor.

A typical wastewater was synthetically prepared by addition of desired amounts of furfural to deionized water. Solution concentrations of 0.5–5 mM l^{-1} or 48–480 ppm were selected. 250–750 ml of synthetic wastewater was introduced to the photoreactor (500 ml if it is not mentioned) and samples were taken every 15 or 30 min. The total run time for batch systems was 120 min. In some experiments hydrogen peroxide as an additional oxidant or sodium oxalate as a reaction accelerator were introduced in low molar rates from 2×10^{-4} to 8×10^{-4} mol h^{-1}.

The floating bed included a bed of 2–5 g coated perlite granules floating on the solution surface and facing the UV source.

Reaction temperature was controlled to be fixed in 28 °C by means of a cooling water flow through the reactor jacket.

2.4. Analysis

Furfural concentration in all samples was analyzed by HPLC analyzing apparatus with a UV absorption detector set at 254 nm for furfural. A Novapack 150 mm × 39 mm i.d. C18 column was used, and the applied mobile phase was 1 ml min^{-1} of gradient chromatography grade acetonitryl and deionized water at a ratio of 60:40.

Perlite granules were analyzed by SEM (JEOL-JXA-840, Japan) and XRD (Bruker D4 XRD analyzer with a Cu Kα X-ray source) before and after coating processes in order to investigate the efficiency of coating process and its effects on attached titania nanoparticles. The results for XRD and SEM analysis are discussed in detail in the previous work of this group [8].

3. Results and discussion

The effects of factors such as, initial concentration of the solution, solution volume, light intensity, molar flow rate of hydrogen peroxide and sodium oxalate, and finally mass of coated perlite granules to surface area ratio, was investigated in this work.

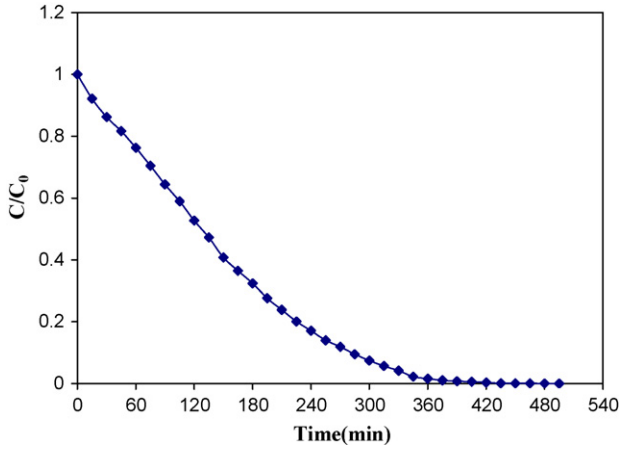

Fig. 2. Function of the reactor in removing furfural from solution.

3.1. Initial concentration

The initial concentration of the solution had a very significant effect on kinetics of the reactions. Kinetics of the reactions follows the known Langmuir–Hinshelwood model. Fig. 2 shows that in concentrations more than 1.6 mM l^{-1}, $C/C_0 > 0.32$, the reaction follows a zero-order kinetic while in lower concentrations it follows a first-order kinetic. Conditions for this experiment was: $C_0 = 5$ mM furfural/l solution; 3 g perlite as the floating bed; 500 ml solution; 125 W UV lamp; aeration to provide required dissolved oxygen.

Table 1 shows removal efficiencies after 120 min for some different initial concentrations.

It was observed that by a decrease in initial concentration, an increase in removal efficiency occurred. This can be caused by less photon absorption by furfural molecules, leading to more catalyst activation and more photolytic degradation of furfural. The maximum absorption wavelength for these molecules is 254 nm, which is found in UV spectrum.

3.2. Solution volume

The volume of the solution in photoreactor also had a significant effect on removal efficiency. The more the solution volume was, the more pollutant molecules needed to be degraded under the same conditions. Moreover, mass diffusion as the controlling step depends on how deep the liquid phase is. The more the solution volume is, the more difficult mass diffusion would be and consequently the less efficient the oxidation process would be. Fig. 3 shows the effect of solution volume on removal efficiency. The experimental conditions for this test included: $C_0 = 0.5$ mM furfural/l solution; 3 g perlite as the floating bed; 125 W UV lamp; aeration to provide required dissolved oxygen.

Table 2 shows the removal efficiencies after 120 min and reaction rate constants for these systems.

3.3. Light intensity

Since the photon flux is a key factor in photochemical reactions and photocatalysts are activated by photons, therefore an increase in reaction rates is expected by an increase in light intensity, however as the light intensities increase, their effects on reaction kinetics decrease so that in high enough intensities no more reaction promotion is observed due to intensity increase. The range of light intensities in this work was not that high, making it possible to investigate the effects of light intensity changes. This phenomenon is shown in Fig. 4. Here the slopes of trend lines are reaction rate constants by considering a first-order reaction kinetic. The reaction rate constant for a 125 W UV source is more than three times the reaction rate constant of a 30 W UV source. In this experiment, reactions took place under these conditions: $C_0 = 0.5$ mM furfural/l solution; 3 g perlite as the floating bed; 500 ml solution; aeration to provide required dissolved oxygen.

Table 3 shows the reaction rate constants and removal efficiencies for these two systems after 120 min.

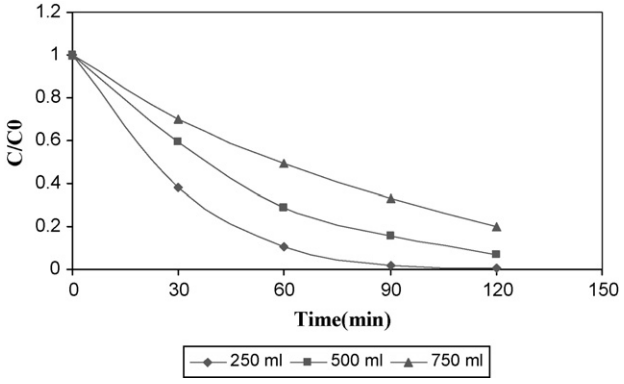

Fig. 3. Solution volume effect.

Table 2
Solution volume effect

Solution volume (ml)	Removal efficiency (%)	Rate constant (min^{-1})
250	99.6	0.0432
500	93	0.0215
750	80	0.0128

$C_0 = 0.5$ mM furfural/l solution; 3 g perlite; 125 W UV lamp; aeration.

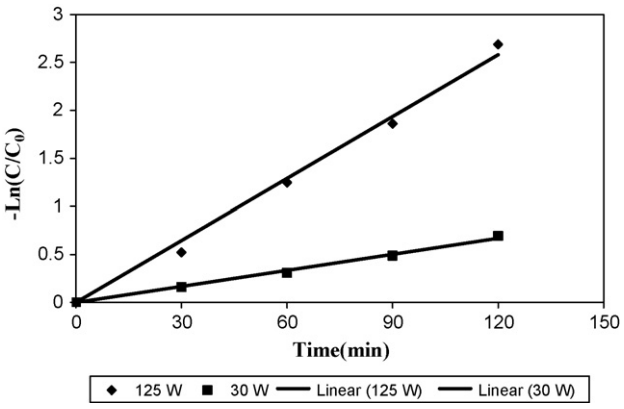

Fig. 4. Light intensity effect.

Table 1
Initial concentration effect

Kinetics	Zero-order					First-order				
Initial concentration (mM l^{-1})	5	4	3.5	3	2	1.6	1	0.7	0.5	0.2
Removal efficiency (%)	47	56	61	66	71	77	89	92	94	97

3 g perlite; 500 ml solution; 125 W UV lamp; aeration.

Table 3
UV source power effect

UV source power (W)	Removal efficiency (%)	Rate constant (min^{-1})
30	50	0.0055
125	93	0.0215

C_0 = 0.5 mM furfural/l solution; 3 g perlite; 500 ml solution; aeration.

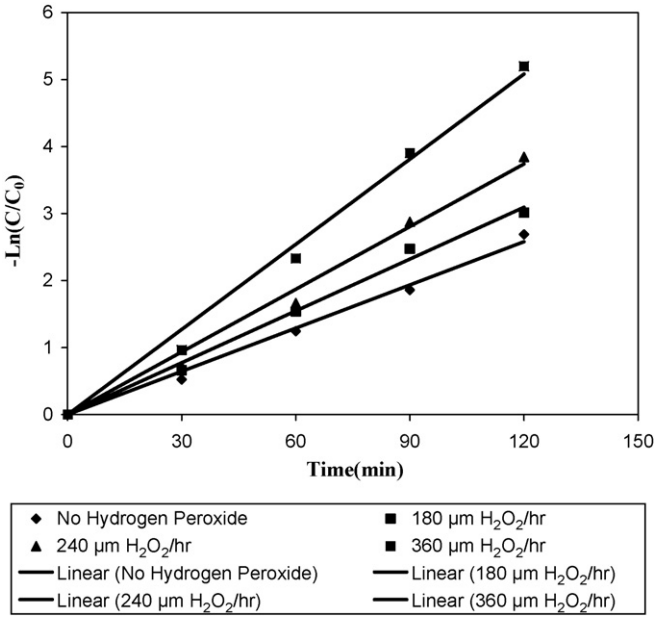

Fig. 5. Hydrogen peroxide effect.

3.4. Hydrogen peroxide molar flow

Besides oxygen as the oxidant, some additional oxidants such as hydrogen peroxide can accelerate reaction rates, in order to investigate the effects of this additional oxidant, some experiments were designed. Experiments revealed that addition of a very low molar flow, for example 360 μmol h^{-1} of hydrogen peroxide could significantly increase the reaction rate by almost twofolds. This is shown in Fig. 5. Conditions for this experiment were: C_0 = 0.5 mM furfural/l solution; 3 g perlite as the floating bed; 500 ml solution; aeration plus hydrogen peroxide to provide required oxidant; 125 W UV lamp.

Table 4 compares the reaction rate constants and removal efficiencies for these four systems after 120 min.

3.5. Oxalate molar flow

Oxalate is a reducing agent, but some experimental evidences in this work proved that it can accelerate the photocatalytic oxidation reactions. This is done by splitting the oxalate ions into its radical forms by UV photons which can convert oxygen molecules to super-oxide radicals and subsequently promoting the oxidation process. Oxalate was introduced in the form of sodium oxalate. Fig. 6 shows how effective this reducing agent could be in promoting an oxidation reaction. These conditions were considered for this experiment: C_0 = 0.5 mM furfural/l solution; 3 g perlite as the floating bed; 500 ml solution; aeration plus sodium oxalate to introduce required reaction promoting agents; 125 W UV lamp.

Table 4
Hydrogen peroxide effect

Hydrogen peroxide molar flow (μmol h^{-1})	Removal efficiency (%)	Rate constant (min^{-1})
0	93	0.0215
180	95	0.0258
240	98	0.0312
360	99.4	0.0424

C_0 = 0.5 mM furfural/l solution; 3 g perlite; 500 ml solution; aeration plus hydrogen peroxide injection; 125 W UV lamp.

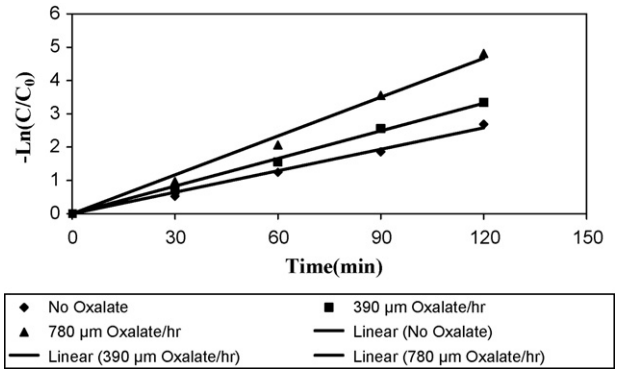

Fig. 6. Sodium oxalate effect.

Table 5
Sodium oxalate effect

Sodium oxalate molar flow (μmol h^{-1})	Removal efficiency (%)	Rate constant (min^{-1})
0	93	0.0215
390	96.5	0.0277
780	99.2	0.0389

C_0 = 0.5 mM furfural/l solution; 3 g perlite; 500 ml solution; aeration plus sodium oxalate; 125 W UV lamp.

Table 5 shows how oxalate ions affect the reaction promotion in these three systems. Removal efficiencies are reported for a retention time of 120 min.

Experiments in this work proved that hydrogen peroxide is much more effective than oxalate in promoting photocatalytic oxidation reactions. Fig. 7 compares two similar systems which used hydrogen peroxide and oxalate in order to accelerate the reaction rate.

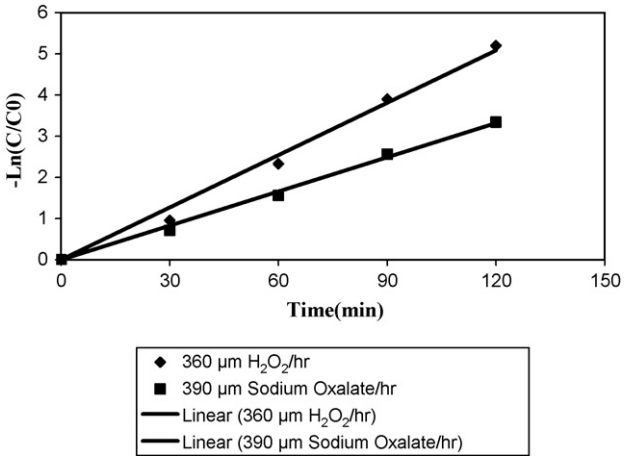

Fig. 7. Comparison of the reactor performance when using hydrogen peroxide or sodium oxalate.

Table 6
Support mass effect

Support mass (g)	Reaction rate constant (min^{-1})
2	0.0202
3	0.0215
4	0.0190
5	0.0174

C_0 = 0.5 mM furfural/l solution; 500 ml solution; 125 W UV lamp; aeration.

3.6. Catalyst mass to solution volume ratio

As expected, catalyst mass was proportional to the process removal efficiency but, there was an optimum catalyst mass for this system. In previous works, especially in slurry type photoreactors, this optimum catalyst mass was due to photon absorption and distraction by catalyst particles and supports near the UV source that made it difficult for farther catalysts obtain enough photon energies. In our floating-bed photoreactor, the optimum catalyst mass in the form of support (perlite granules) mass corresponded the minimum mass of support coated with catalyst which can cover the whole solution surface, because additional supports would accumulate below the upper support layer, adsorbing the substrate while the upper support layer adsorbed the photons not leaving enough photons for the layer below. Table 6 shows the observed reaction rate constants by considering a first order kinetic for the reactions. It was revealed that this optimum support mass was 3 g for the surface area of the photoreactor used in this work. All systems were similar with different support mass.

3.7. Kinetics

Experimental data in this work supported the idea that kinetics of these photocatalytic reactions followed the Langmuir–Hinshelwood model.

By splitting the curve in Fig. 2, it was revealed that for concentrations more than 1.6 mM l^{-1}, the reaction follows a zero-order kinetic. The slope of trend line in Fig. 8, corresponds k_{obs}/C_0 value which suggests an observed reaction rate constant (k_{obs}) of 0.0195 mM min^{-1} for C_0 = 5 mM l^{-1}.

Fig. 9 shows that in concentrations less than 0.6 mM l^{-1}, a first-order reaction kinetic is observed. This chart is based on the data obtained from Fig. 2, by considering C_0 = 0.6 mM l^{-1} which corresponds to C/C_0 = 0.12 in Fig. 2. The equation at the corner of the figure, applies for the equation of a first-order reaction with a rate constant of 0.0221 min^{-1}.

When the initial concentration was set to be 0.3 mM l^{-1} and what we did in the last step was repeated, Fig. 10 was obtained which suggests a better fitness to first-order reactions with a rate constant of 0.0274 min^{-1}.

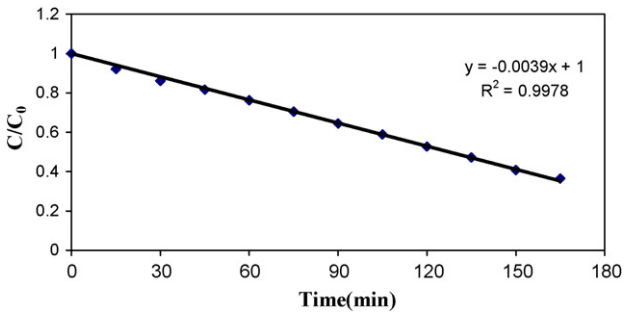

Fig. 8. Behavior of the reaction for C_0 = 5 mM furfural/l solution.

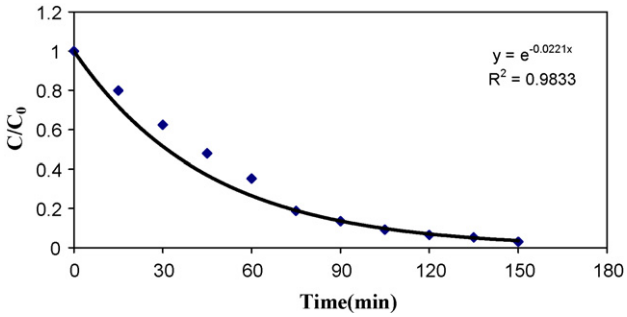

Fig. 9. Behavior of the reaction for C_0 = 0.6 mM furfural/l solution.

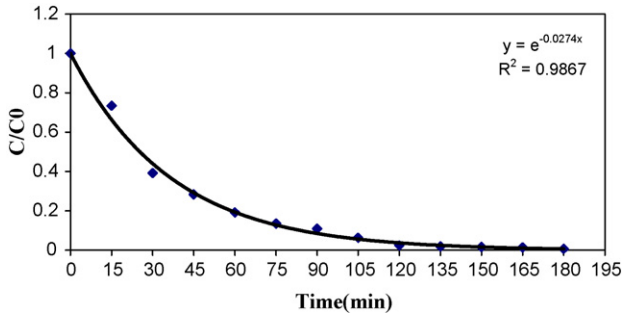

Fig. 10. Behavior of the reaction for C_0 = 0.3 mM furfural/l solution.

Table 7 shows the behavior of reactions by changing the initial concentration. Regression factors and rate constants for curve fitting to first-order reactions are shown in Table 7.

There were some factors such as light intensity that could change the initial concentrations at which the order of the reactions changed; for example, if a 30 W UV source was used to treat a solution with an initial concentration of 0.5 mM l^{-1}, the reaction showed both a zero-order and a first-order reaction behavior, while the same system with a 125 W UV source showed a behavior far from a zero-order reaction kinetic. Fig. 11 shows this difference.

3.8. The amount of catalyst immobilized on perlite granules

The amount of catalyst immobilized in five separate catalyst immobilization experiments was determined to be 0.121, 0.130, 0.124, 0.119 and 0.134 g catalyst on 1 g perlite/catalyst system, 0.126 g catalyst on 1 g perlite/catalyst system on average.

Table 7
Initial concentration effect

Initial concentration (mM l^{-1})	Regression factor (R^2)	Reaction rate constant (min^{-1})
0.6	0.9833	0.0221
0.48	0.9854	0.0252
0.37	0.9874	0.0263
0.3	0.9867	0.0274
0.21	0.9817	0.0283
0.11	0.9772	0.0262
0.081	0.9725	0.0271
0.055	0.9633	0.0273
0.039	0.949	0.0281
0.031	0.8991	0.0313
0.018	0.8349	0.0293

3 g perlite; 500 ml solution; 125 W UV lamp; aeration.

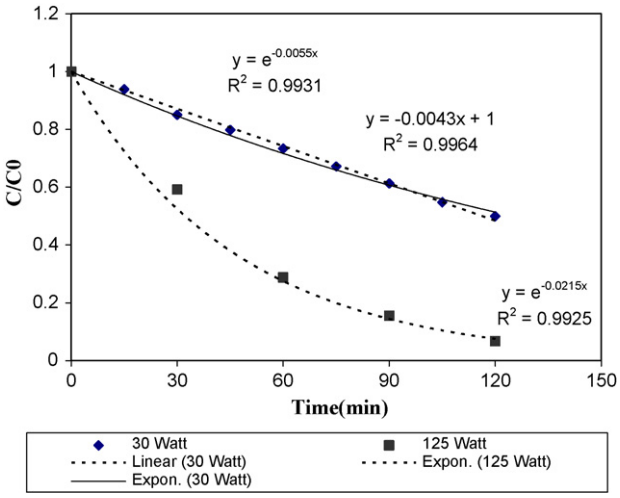

Fig. 11. Reaction behavior for different light intensities.

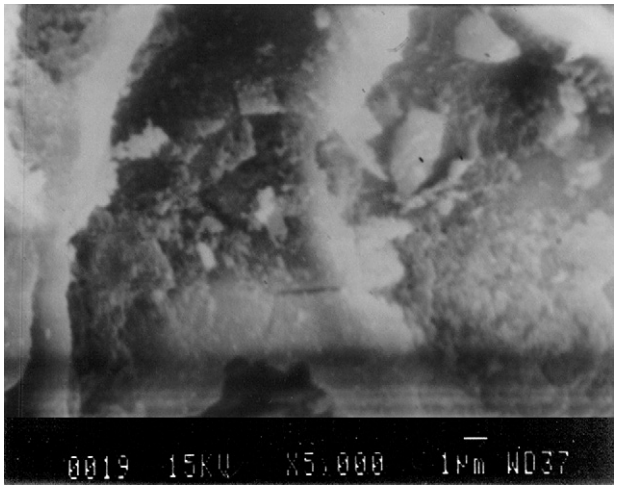

Fig. 12. Perlite granule coated with titanium dioxide.

Fig. 12 shows titanium dioxide particles immobilized on a perlite granule. The image is rather obscure but the catalyst particles can be identified revealing the fact that the immobilization technique was successful. In order to compare coated and uncoated perlite granules Fig. 13 can be helpful, this image shows an uncoated perlite granule.

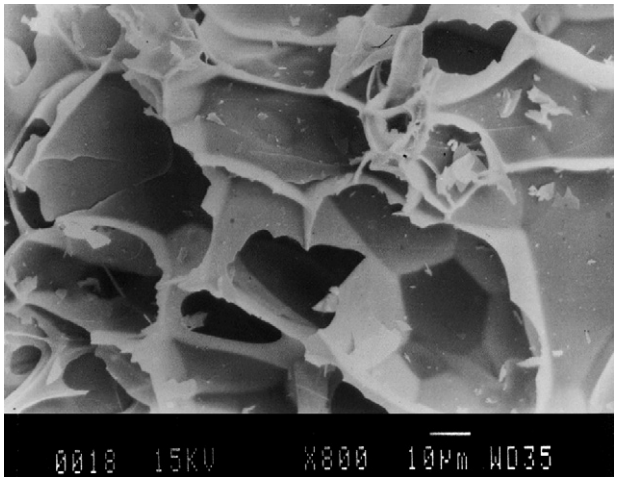

Fig. 13. Uncoated perlite granule.

4. Conclusions

Photocatalytic oxidation turned out to be a good and promising process to purify solutions polluted by furfural, especially in low concentrations. This was an inexpensive, easy to run, effective and fast process by which removal efficiencies more than 95% could be achieved in just 2 h. Using additional oxidants especially hydrogen peroxide even in very low molar flows of a few hundred micromoles per hour, the removal reaction rates rose to more than twofolds. The floating bed photoreactor used in this work appeared to be a proper system with a good efficiency due to the ability of photons to penetrate more efficiently and more energetically through air instead of water to face the catalyst in order to purify this kind of wastewater.

Kinetics of the reactions involved, followed the Langmuir–Hinshelwood model. Initial concentration showed to be essential in determining the order of the reaction and light intensity appeared to affect the concentration at which the order of the reaction shifts. The XRD and SEM analysis on coated perlite granules revealed that the method adopted to immobilize titanium dioxide nanoparticles on perlite granules was suitable for this purpose. No serious structural changes were detected in titanium dioxide particles and distribution of anchored titania on perlite surface was uniform.

References

[1] K. Kabra, R. Chaudhary, R.L. Sawhney, Treatment of hazardous organic and inorganic compounds through aqueous-phase photocatalysis: a review, Ind. Eng. Chem. Res. 43 (2004) 7683.
[2] M. Hamerski, J. Grzechulska, A.W. Morawski, Photocatalytic purification of soil contaminated with oil using modified TiO_2 powders, Solar Energy 66 (1999) 395.
[3] M.M. Higarashi, W.F. Jardim, Remediation of pesticide contaminated soil using TiO_2 mediated by solar light, Catal. Today 76 (2002) 201.
[4] Q. Huang, C.S. Hong, TiO_2 photocatalytic degradation of PCBs in soil-water systems containing fluoro surfactant, Chemosphere 41 (2000) 871.
[5] A.J. Maira, J.M. Coronado, V. Augugliaro, K.L. Yeung, J.C. Conesa, J. Soria, Fourier transform infrared study of the performance of nanostructured TiO_2 particles for the photocatalytic oxidation of gaseous toluene, J. Catal. 202 (2001) 413.
[6] J. Medina-Valtierra, J. García-Servín, C. Frausto-Reyes, S. Calixto, The photocatalytic application and regeneration of anatase thin films with embedded commercial TiO_2 particles deposited on glass microrods, Appl. Surf. Sci. 252 (2006) 3600.
[7] X. Zhao, X. Quan, H. Zhao, S. Chen, Y. Zhao, J. Chen, Different effects of humic substances on photodegradation of *p,p′*-DDT on soil surfaces in the presence of TiO_2 under UV and visible light, J. Photochem. Photobiol. A: Chem. 167 (2004) 177.
[8] S.N. Hosseini, M. Vosoughi, M. Borghei, Immobilization of TiO_2 on perlite granules for photocatalytic degradation of phenol, Appl. Catal. B: Environ. 74 (2007) 53–62.
[9] M. Lewandowski, D.F. Ollis, Halide acid pretreatments of photocatalysts for oxidation of aromatic air contaminants: rate enhancement, rate inhibition, and a thermodynamic rationale, J. Catal. 217 (1) (2003) 38–46.
[10] O. d'Hennezel, P. Pichat, D.F. Ollis, Benzene and toluene gas-phase photocatalytic degradation over H_2O and HCl pretreated TiO_2: by-products and mechanisms, J. Photochem. Photobiol. A: Chem. 118 (3) (1998) 197–204.
[11] F. Thevenet, O. Guaïtella, J.M. Herrmann, A. Rousseau, C. Guillard, Photocatalytic degradation of acetylene over various titanium dioxide-based photocatalysts, Appl. Catal. B: Environ. 61 (1–2) (2005) 58–68.
[12] I. Bouzaida, C. Ferronato, J.M. Chovelon, M.E. Rammah, J.M. Herrmann, Heterogeneous photocatalytic degradation of the anthraquinonic dye, Acid Blue 25 (AB25): a kinetic approach, J. Photochem. Photobiol. A: Chem. 168 (1–2) (2004) 23–30.
[13] M. Karkmaz, E. Puzenat, C. Guillard, J.M. Herrmann, Photocatalytic degradation of the alimentary azo dye amaranth: mineralization of the azo group to nitrogen, Appl. Catal. B: Environ. 51 (3) (2004) 183–194.
[14] S. Malato, J. Blanco, A. Campos, J. Cáceres, C. Guillard, J.M. Herrmann, A.R. Fernández-Alba, Effect of operating parameters on the testing of new industrial titania catalysts at solar pilot plant scale, Appl. Catal. B: Environ. 42 (4) (2003) 349–357.

[15] C. Adán, A. Bahamonde, A. Martínez-Arias, M. Fernández-García, L.A. Pérez-Estrada, S. Malato, Solar light assisted photodegradation of ethidium bromide over titania-based catalysts, Catal. Today 129 (1–2) (2007) 79–85.
[16] L.A. Pérez-Estrada, A. Agüera, M.D. Hernando, S. Malato, A.R. Fernández-Alba, Photodegradation of malachite green under natural sunlight irradiation: kinetic and toxicity of the transformation products, Chemosphere 70 (2008) 2068–2075.
[17] P. Fernández, J. Blanco, C. Sichel, S. Malato, Water disinfection by solar photocatalysis using compound parabolic collectors, Catal. Today 101 (3–4) (2005) 345–352.
[18] Advanced Photochemical Oxidation Processes, EPA Press, Office Of Research And Development, Washington, DC, United States, 1998.
[19] J.B. Galvez, Solar Detoxification, United Nations Educational, Scientific and Cultural Organization (UNESCO), 2003.
[20] F. Haque, E. Vaisman, C.H. Langford, A. Kantzas, Preparation and performance of integrated photocatalyst adsorbent (IPCA) employed to degrade model organic compounds in synthetic wastewater, J. Photochem. Photobiol. A: Chem. 169 (2005) 21–27.
[21] J. Matos, J. Laine, J.-M. Herrmann, D. Uzcategui, J.L. Brito, Influence of activated carbon upon titania on aqueous photocatalytic consecutive runs of phenol photodegradation, Appl. Catal. B: Environ. 70 (1–4) (2007) 461–469.
[22] J. Matos, J. Laine, J.-M. Herrmann, Effect of the type of activated carbons on the photocatalytic degradation of aqueous organic pollutants by UV-irradiated titania, J. Catal. 200 (1) (2001) 10–20.
[23] A. Fernández, G. Lassaletta, V.M. Jiménez, A. Justo, A.R. González-Elipe, J.-M. Herrmann, H. Tahiri, Y. Ait-Ichou, Preparation and characterization of TiO_2 photocatalysts supported on various rigid supports (glass, quartz and stainless steel). Comparative studies of photocatalytic activity in water purification, Appl. Catal. B: Environ. 7 (1–2) (1995) 49–63.
[24] M. Walter, M. Ruger, C. RagoX, G.C.M. Steffens, D. Hollander, O. Paar, R.H. Maier, W. Jahnen-Dechent, A. Bosserhoff, H. Erli, In vitro behavior of aporous TiO_2/perlite composite and its surface modification with fibronectin, Biomaterials 26 (2005) 2813–2826.
[25] Furfural safety data sheet, based on directive 2001/58/EC of the commission of the European communities.